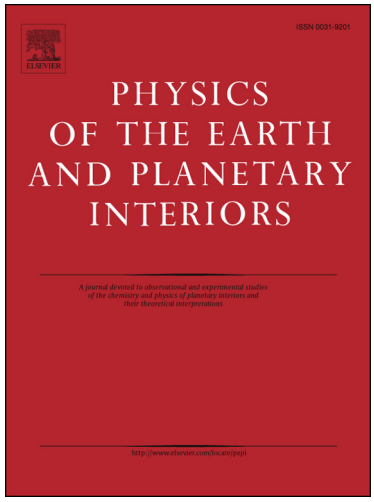

P–V–T equation of state of Na-majorite to 21 GPa and 1673 K

Anna M. Dymshits, Konstantin D. Litasov, Anton Shatskiy, Igor S. Sharygin, Eiji Ohtani, Akio Suzuki, Nikolay P. Pokhilenko, Kenichi Funakoshi

PII: S0031-9201(13)00164-7
DOI: http://dx.doi.org/10.1016/j.pepi.2013.11.005
Reference: PEPI 5674

To appear in: *Physics of the Earth and Planetary Interiors*

Please cite this article as: Dymshits, A.M., Litasov, K.D., Shatskiy, A., Sharygin, I.S., Ohtani, E., Suzuki, A., Pokhilenko, N.P., Funakoshi, K., *P–V–T* equation of state of Na-majorite to 21 GPa and 1673 K, *Physics of the Earth and Planetary Interiors* (2013), doi: http://dx.doi.org/10.1016/j.pepi.2013.11.005

P – V – T equation of state of Na-majorite to 21 GPa and 1673 K

Anna M. Dymshits [a,*], Konstantin D. Litasov [a,b], Anton Shatskiy [a,b], Igor S. Sharygin [a], Eiji Ohtani [c], Akio Suzuki [c], Nikolay P. Pokhilenko [a], Kenichi Funakoshi [d]

[a] V.S. Sobolev Institute of Geology and Mineralogy, Siberian Branch of Russian Academy of Science, Novosibirsk, 630090, Russia

[b] Novosibirsk State University, Novosibirsk, 630090, Russia

[c] Department of Earth and Planetary Materials Science, Graduate School of Science, Tohoku University, Sendai 980-8578, Japan

[d] SPring-8, Japan Synchrotron Radiation Research Institute, Kouto, Hyogo 678-5198, Japan

* Corresponding author.

E-mail address: A.Dymshits@gmail.com

tel./fax +7(383)3332792

Abstract

The *P–V–T* equation of state (EoS) for Na-majorite (Na-maj) at pressures to 21 GPa and temperatures to 1673 K was obtained from *in situ* X-ray diffraction experiments using a Kawai-type multi-anvil apparatus. Analyses of the room-temperature *P–V* data to a third-order Birch–Murnaghan EoS yielded ambient unit cell volume, V_0 = 1476 (1) (Å^3); isothermal bulk modulus, $K_{0,300}$ = 181 (9) GPa; and its pressure derivative, $K'_{0,300}$ = 4.4 (1.2). When fitting a high-temperature Birch–Murnaghan EoS using entire *P–V–T* data at a fixed V_0 = 1475.88 Å^3, $K_{0,300}$ = 184 (4) GPa, $K'_{0,300}$ = 3.8 (6), $(\partial K_{0,T}/\partial T)_P$ = -0.023 (5) (GPa K^{-1}), and a = 3.17 (16) × 10^{-5} K^{-1}, b = 0.16 (26) × 10^{-8} K^{-2}, where $\alpha = a + bT$ is the volumetric thermal expansion coefficient. Fitting the Mie–Grüneisen–Debye (MGD) EoS with the present data to Debye temperature fixed at θ_0 = 890 K yielded Grüneisen parameter, γ_0 = 1.35 at q = 1.0 (fixed). The new data on Na-majorite were compared with the previous data on majorite type garnets. The entire dataset enabled to examine the thermoelastic properties of important mantle garnets and these data will have further applications for modeling *P – T* conditions in the transition zone of the Earth's mantle using ultradeep mineral assemblages.

Key words: Na-majorite; Equation of state; X-ray diffraction; High pressure experiment

1. Introduction

Garnet is one of the most abundant mineral in the upper mantle and transition zone and can comprise up to 40 vol.% of peridotitic and up to 70 vol.% of basaltic or eclogitic lithologies (Akaogi and Akimoto, 1977; Anderson and Bass, 1984; Irifune and Ringwood, 1987; Ita and Stixrude, 1992). With increasing pressure garnet becomes progressively depleted in Al and Cr while the Si content in octahedral site, as well as concentrations of the divalent cations (Ca, Mg, Fe) and Na, regularly increase (Fig. 1). Na admixture (up to 0.22 wt.%) was originally discovered in pyrope garnets from eclogite xenoliths and inclusions in diamonds derived by Siberian kimberlites, as well as in UHP complexes and inclusions in diamonds (Sobolev and Lavrent'ev, 1971). The authors suggested direct connection between the sodium concentrations and the six-coordinated silicon that can be expressed as a function of pressure. Later, Gasparik (1989) documented many high-silicon garnets, including a sample close to the end-member composition of $Na_2MgSi_5O_{12}$ (Na-maj). Recently, Bobrov et al. (2008a; 2008b) and Dymshits et al. (2013) experimentally demonstrated that the amount of sodic component in garnet may significantly increase with pressure. Thus, it can be used as the pressure marker for mineral assemblages with Na-majoritic garnets at the conditions of the deep upper mantle and transition zone. Moreover, due to the complex composition of natural garnets, which can widely vary depending on the conditions (Harte, 2010; Kiseeva et al., 2013), the study of the thermoelastic properties of end-member garnets is an important key to understand the processes occurring at high pressures and temperatures in the mantle. Mineral assemblages with majoritic garnet are of special importance, because they can crystallize under the conditions of deep upper mantle and transition zone (Stachel, 2001). Methods of depth estimation with account for the composition of majoritic garnet were developed by Stachel (2001), Collerson (2010), and Simakov and Bobrov (2008). Experimentally obtained dependence of Na and Si contents (Na-maj component) in garnet on pressure should be taken into account for the calculation of improved geobarometers for majorite-bearing mineral assemblages (Harte, 2010; Kiseeva et al., 2013). Collerson et al. (2010) have derived a tools for empirical estimation of pressure in natural garnets based on both the coupled substitution $(Na+)^{[1+]}(Ti + {}^{[VI]}Si)^{[4+]} = (M)^{[2+]}(Al + Cr)^{[3+]}$, and the classic pyroxene-stoichiometry majorite-substitution. In this equation sodium can be expressed as Na-majorite component. To improve the approach suggested by Collerson more thermodynamic parameters of Na-majorite and Na-pyroxene (Na-px) are needed. However, thermodynamic data for Na-maj as well as its mixing properties have been poorly determined. The crystal structure of Na-maj has been studied at ambient conditions (Pacalo et al., 1992; Bindi et al., 2011) and at high pressures and temperatures by atomistic modeling (Vinograd et al., 2011). The compressibility curve was studied at ambient temperature by Hazen et al. (1994) . Hazen et al. (1994) investigated compressibility of synthetic Na-maj $[(Na_{1.88}Mg_{1.12})(Mg_{0.06}Si_{1.94})Si_3O_{12}]$ by single-crystal

X-ray diffraction using Merrill-Bassett diamond anvil cell up to 5 GPa. The obtained value of 191.5 ± 2.5 GPa for isothermal bulk modulus differs significantly from the adiabatic bulk modulus measured at ambient conditions using Brillouin spectroscopy for the same composition, which was 173.5 GPa (Pacalo et al., 1992). We can emphasize that crystal analyzed by Pacalo et al. (1992) have some amount of majorite that has bulk modulus close to 163 GPa (Hunt et al., 2010). It means that the value forpure Na-maj would be higher than one obtained by Pacalo et al. (1994). The discrepancies between two studies for the crystals of the same composition were explained by Hazen et al. (1994) as the result of the assumption for $K'_{0,300} = 4$. Being greater than 5, $K'_{0,300}$ reduces bulk modulus to the value below 190 GPa. However, Hazen et al. (1994) obtained only 8 experimental points at room temperature that is not enough for the accurate refinement of the bulk modulus. Here, we present pressure− volume− temperature relations for synthetic Na-maj by means of multi-anvil press experiments combined with X-ray diffraction at pressures to 21 GPa and temperatures to 1673 K. A complete set of the thermoelastic parameters for *PT*-conditions of the transition zone are extracted using various equations of state and discussed by comparing with those of the previous studies.

2. Experimental procedure and sample description

The starting material was a gel of $Na_2MgSi_5O_{12}$ prepared using the nitrate gelling method (Hamilton and Henderson, 1968). The starting material was mixed with 5 wt.% Au powder used as pressure marker.

In situ X-ray diffraction experiment #P187 was conducted at the Photon Factory (Tsukuba, Japan), using a 700-tons Kawai-type multi-anvil apparatus "MAX-III" installed at a bending magnet beamline NE7A (Suzuki et al., 2011). We used 22 mm WC anvils (Tungaloy F-grade) with a truncated edge length of 3.5 mm. The sample assembly was essentially the same with that used in (Litasov and Ohtani, 2009) but modified for the *in situ* study (Fig.2). It consisted of a ZrO_2 pressure medium, a cylindrical $LaCrO_3$ heater, molybdenum electrodes, and a BN sample capsule. Temperature was monitored by a $W_{25\%}Re-W_{3\%}Re$ thermocouple with a junction located at nearly the same position as where the X-ray path through the sample. Runs #M1127 and #S2683 were conducted at the "SPring-8" synchrotron radiation facility (Hyogo, Japan), using a 1500-tons Kawai-type multi-anvil apparatus, "Speed-Mk.II" and "SPEED-1500", installed at a bending magnet beam line BL04B1 (Utsumi et al., 1998). We also used oscillation system installed in SPEED-Mk.II to prevent the peak disappearance from the diffraction (Katsura et al., 2004) because of the crystal growth. This system was quite successful to get ideal diffraction pattern in spite of the limitation of the oscillation angle (6°). The design of cell assembly was the same with described above for Run #P187.

The experimental setup is explained in details in Litasov et al. (2013). Experiments were performed at 3-21 GPa and 300-1673 K (Fig.3; Table 1). The cell assembly was first compressed to desired press load at ambient temperature. Thereafter, we followed a complex *PT*-path with 2 or 3 heating/decompression circles (Fig. 3) while continuously taking diffraction patterns. Typical exposure time for collecting diffraction data were 200-400 s.

Representative X-ray diffraction patterns are shown in Fig. 4 illustrating diffraction peaks of Na-maj, stishovite, and Au pressure marker. The experimental pressures were calculated from the unit cell volume of Au using the equation of state (EoS) from (Dorogokupets and Dewaele, 2007; Sokolova et al., 2013). Typically, 4-5 of the diffraction lines [(1 1 1), (2 0 0), (2 2 0), (3 1 1), and (2 2 2)] of Au were used to calculate the pressures, and about 8-10 diffraction lines were used to calculate the volume of Na-maj (Fig. 4). Refinement of peaks positions and determination the *d*-values were achieved using the XRayAnalysis software provided by beam line. The refinement of weak individual and some overlapped peaks were re-examined manually. The uncertainties of unit cell volume of Au, determined by least-square method, give typically 0.1 GPa uncertainty in pressure. The unit cell volume of Na-maj was calculated using the UnitCell software (Holland and Redfern, 1997).

The recovered samples were examined with an electron microprobe (JEOL Superprobe JXA-8800) at Tohoku University. An acceleration voltage of 15 kV and 10 nA specimen current was used for the analyses. The compositions of recovered garnets were slightly deviated from stoichiometry to be $Na_{1.90}Mg_{1.00}Si_{5.00}O_{12}$ due to loss of sodium under electron beam. The consistency of synthesized garnet compositions were confirmed by relevant consistency of calculated $P-V-T$ data in different runs.

3. Results and discussion

3.1. Pressure – volume data at room temperature

The unit cell parameters of Na-maj obtained after experiment #P187 at ambient conditions are a = 11.3855 (4) Å and V_0 = 1475.88 (16) Å^3. The cell volume is slightly larger than that obtained by single crystal observations, 1472.5 Å^3 (Bindi et al., 2011). The cell parameters reported by Hazen et al. (1994) and Pacalo et al. (1992) are around 1485.5 Å^3 that is about 0.7% larger than that obtained in the present study. The unit cell parameter and volume of Na-maj are lower than those for any other garnet end members (Milman et al., 2001; Chopelas, 2006). As it was demonstrated by Bindi et al. (2011), Na and Mg are disordered at the X site, whereas both Y (octahedral) and Z (tetrahedral) sites are occupied by silicon. Passing from pure pyrope to pure Na-majorite we observe the substitution of Si for Al in Y site. The difference in their size is significant that may cause decrease of the Y site distances relative to pyrope (1.79 Å and 1.85 Å, respectively). At the same time, transition from an X site fully occupied

with Mg to a mixed (Na, Mg) population results in the slight increase of the X-O distances (from 2.28 Å to 2.31 Å). As a result, a decrease of the unit-cell parameters is observed from pure pyrope to Na-majorite.

The pressure− volume relations have been determined at 300 K from 0 to 17 GPa by fitting the experimental data to a third-order Birch− Murnaghan (BM) EoS:

$$P(V,300) = 1.5K_{0,300}\left[\left(\frac{V_{0,300}}{V_{P,300}}\right)^{7/3} - \left(\frac{V_{0,300}}{V_{P,300}}\right)^{5/3}\right] \times \left[1 - 0.75(4 - K'_{0,300})\left(\left(\frac{V_{0,300}}{V_{P,300}}\right)^{2/3} - 1\right)\right] \quad (1)$$

where $V_{0,300}$, $K_{0,300}$ and $K'_{0,300}$ are unit-cell volume, isothermal bulk modulus and its pressure derivative at ambient condition, respectively. When K_T' is fixed to 4, the fitting to BM EoS gives $K_{0,300}$ = 184 (3) and V_0 = 1476 (1) Å^3. Adiabatic bulk modulus measured at ambient conditions using Brillouin spectroscopy gives relatively low value, $K_{S,0}$ = 173.5 GPa (Pacalo et al., 1992) that is close to grossular garnet (Gréaux et al., 2011). It appears to connect with $Mg_4Si_4O_{12}$ admixture in that garnet (Pacalo et al., 1992; Hazen et al., 1994). The fitting of Eq. 1 to the data with all parameters variable yields V_0 = 1476 (1) Å^3, $K_{0,300}$ = 181 (9) GPa, and $K'_{0;300}$ = 4.4 (1.2) and gives the values of $K_{0,300}$ = 180 (5) GPa and $K'_{0;300}$ = 4.5 (9) for the V_0 fixed at 1475.88 Å^3. Both calculations are closely agreed with each other. Since the fitted $V_{0,300}$ is the same as the measured values within the errors it is suitable to fix $V_{0,300}$ at 1475.9 Å^3 in the all following fittings procedures.

The obtained $P-V$ relations differ slightly from those previously reported for garnets referred in literature as Na-maj (Table 2). The discrepancy between the parameters obtained by Hazen et al. (1994) and in the present work can be explained by insufficiency of experimental data points for accurate refinement. The present pressure–relative volume relation of Na-maj agrees well with those of Hazen et al. (1994) (fig. 5). It means that the real bulk modulus of the garnet obtained by Hazen et al. (1994) can be lower.

Milman et al. (2001) showed that the bulk modulus of garnet is strongly affected by the bulk modulus of the dodecahedra, while compressibility of other individual polyhedra displays no correlation with the compressibility of the structure as a whole. If so, Na-maj would have the smallest bulk modulus of all silicate garnets, as a phase with a predicted dodecahedral bulk modulus of approximately 70 GPa (Hazen et al., 1994). In fact Na-maj has the largest bulk modulus among the silicate garnets. This behavior must reflect the all-mineral framework of Na-maj with very small cell volume and silicon in the octahedral position. Thus, we conclude that not only the dodecahedral sites, but also the behavior of the garnet framework and relative sizes of the 8- and 6-coordinated cations, control garnet compression. The octahedral site in Na-maj is quite small (1.79 Å) and contains only silicon in comparison to the pyrope (1.85 Å) or majorite (1.88 Å). The small and highly charged octahedra share four edges with the dodecahedra and thus restrict the volume of the large and low charged

dodecahedra. In spite Na-maj has a large average X-cation radius (R_{Na} = 1.07 Å) its dodecahedral volume is relatively small (V = 21.23 and 21.26 Å^3) (Bindi et al., 2011).

As it was shown by Milman et al. (2001) there are two major compression mechanisms for garnets. One of them is the bond compression, another is the bond bending. The more efficient compression can take place in XO_8 dodecahedra and YO_6 octahedra and would appear as a result of polyhedra rotation. Pacalo et al. (1992) suggested that XO_8 polyhedra act as braces and controls the amount of rotation between tetrahedra and octahedra within the corner-linked chains. In case of pyrope XO_8 cite is not filled up and polyhedra within the corner-linked chains can rotate freely to accommodate applied stress. In case of Na-maj the dodecahedral site is filled up and rotational freedom is minimized. Such relations between the XO_8 and YO_6 sites provide evidence for comparatively more rigid structure. As a result, Na-maj with all octahedral sites occupied by silicon has the largest value of the bulk modulus among garnets. It would be interesting to study compressibility of Li-majorite expressed by Yang et al. (Yang et al., 2009). That phase has smaller cell volume (1430 Å^3) and X-O distance (2.26 Å) but the same YO_6 polyhedra fully occupied by silicon.

3.2. P – V – T data and thermoelastic parameters

Pressure–volume–temperature data were used to determine the thermoelastic properties of Na-majorite with two different approaches: the high-temperature Birch–Murnaghan (HTBM) EoS and the Mie–Grüneisen–Debye (MGD) EoS.

The third-order Birch– Murnaghan EoS is given by following expression for *P(V,T)*:

$$P(V,T) = 1.5K_{0,T}\left[\left(\frac{V_{0,T}}{V_{P,T}}\right)^{7/3} - \left(\frac{V_{0,T}}{V_{P,T}}\right)^{5/3}\right] \times \left[1 - 0.75(4 - K'_{0,300})\left(\left(\frac{V_{0,T}}{V_{P,T}}\right)^{2/3} - 1\right)\right] \quad (2)$$

In the HTBM EoS the temperature effect on $K_{0,T}$ can be expressed as a linear function of temperature, temperature derivative $(\partial K_{0,T}/\partial T)_P$ and $K_{0,300}$ as follows:

$$K_{0,T} = K_{0,300} + \left(\frac{\partial K_{0,T}}{\partial T}\right)_P \times (T - 300) \quad (3)$$

The temperature dependence of the volume at ambient pressure $V_{0,T}$ can be expressed as a function of the thermal expansion at zero-pressure, $\alpha_{0,T} = a + bT$:

$$V_{0,T} = V_{0,300}\exp\left[\int_{300}^{T} \alpha_{0,T}\,dT\right] = V_{0,300}\exp\left(a(T - 300) + \frac{1}{2}b(T^2 - 300^2)\right) \quad (4)$$

In this approach we can obtain six parameters V_0, $K_{0,300}$, $K'_{0,300}$, $(\partial K_{0,T}/\partial T)$, a and b by a least squares fit. The calculated parameters are listed in Table 2. The results of the fit of Na-maj are compared to previous studies on majorite-type garnets for a set of different fixed $K'_{0,300}$ values (Table 2). When there is no constraint applied on the elastic parameters, fitting of Eq. 2 gives V_0 = 1475.4 (1.2) Å^3, $K_{0,300}$ = 186 (6) GPa, $K'_{0,300}$ = 3.6 (7), $(\partial K_{0,T}/\partial T)$ = -0.023 (5) GPa K^{-1}, a = 3.17 (16) × 10^{-5} K^{-1}, and b = 0.16 (26) × 10^{-8} K^{-2} that are of the same order of those obtained with the fixed V_0 = 1475.9 Å^3. The

bulk modulus and its pressure derivative agree well with the values fitted by room temperature BM EoS taking the uncertainties into account. In this calculation the uncertainties in the bulk modulus and its first pressure derivative are quite large. This indicates that our data are not sufficient to constrain all the elastic parameters at the same time during fitting. Thus, fitting the HTBM EoS with the V_0 = 1475.9 Å^3 (Fig. 6) yields more realistic parameters: $K_{0,300}$ = 184 (3) GPa, $K'_{0,300}$ = 3.8 (6), $(\partial K_{0,T}/\partial T)$ = -0.023 (5) GPa K^{-1}, a = 3.18 (16) × 10^{-5} K^{-1}, and b = 0.18 (21) × 10^{-8} K^{-2} . The value of thermal expansion is close to andradite.

Studies with laser induced phonon spectroscopy (Brillouin scattering and impulsively stimulated scattering) on garnets at high-pressures generally result in $K'_{0,300}$ ~ 4, whereas studies with ultrasonic interferometry at high-pressures corresponds to higher values for $K'_{0,300}$ ~ 5– 6.5 (i.e. (Gwanmesia et al., 2000; Sinogeikin and Bass, 2002). If $K'_{0,300}$ is fixed to 4.0 we obtain $K_{0,300}$ = 182.1 (9), $(\partial K_{0,T}/\partial T)$ = -0.025 (3) GPa K^{-1} and a = 3.20 (14) × 10^{-5} K^{-1} and b = 0.24 (20) × 10^{-8} K^{-2}. The bulk modulus measured at ambient conditions using Brillouin spectroscopy gives the value close to our fitting with $K'_{0,300}$ fixed at 5.0. Figure 7 shows that the temperature dependences of bulk modulus $(\partial K_{0,T}/\partial T)_P$ for Na-maj at any $K'_{0,300}$ is much higher than for majorite or pyrope and similar to almandine type garnet at $K'_{0,300}$ = 5.0. Moreover the present synthetic Na-majorite softens faster against temperature compared to other garnets. The value of $(\partial K_{0,T}/\partial T)$ is moderately affected by the variations of $K'_{0,300}$ and varies from -0.023 to -0.031 GPa K^{-1}. However, the $K_{0,300}$ values changes significantly because of the strong correlation between the bulk modulus and $K'_{0,300}$ (Table 2). Thus, it is reasonable to suggest that a consistent set of parameters can be obtained by fixing all values from the room temperature BM EoS, which gives $\alpha_{0,T}$ = 3.31 (20) × 10^{-5} K^{-1} and $(\partial K_{0,T}/\partial T)$ = -0.029 (3) GPa K^{-1}. In reality the fitting with the only V_0 fixed and other 5 parameters variables provided the minimum root mean square (RMS) misfit for pressure values ($P_{obs} - P_{cal}$). The thermal expansion $\alpha_{0,T}$ derived from that fitting are larger than that for other majorite type garnets.

In the MGD EoS (Jackson and Rigden, 1996) the pressure is described by the sum of the static pressure at room temperature $P(V,300)$ and the thermal pressure $\Delta P_{\mathrm{th}}(V,T)$.

$$P(V,T) = P(V,300) + \Delta P_{\mathrm{th}}(V,T) \quad (5)$$

The third order Birch– Murnaghan equation (Eq. 1) with V_0 fixed during the calculations and Mie– Grüneisen relations are used to express the static pressure $P(V,300)$ and the thermal pressure $\Delta P_{\mathrm{th}}(V,T)$, respectively.

The thermal pressure is a function of the Grüneisen parameter γ and the thermal energy $E_{\mathrm{th}}(V, T)$, that can be estimated using a Debye model:

$$\Delta P_{Th}(V,T) = \frac{\gamma\,(V,T)}{\mathrm{V}}\left[\mathrm{E_{th}}(V,T) - \mathrm{E_{th}}(V,T_0)\right] \quad (6)$$

$$\mathrm{E}_{th}(V,T) = \frac{9\mathrm{nRT}}{(\theta/\mathrm{T})^3}\int_0^{\theta/\mathrm{T}} \frac{\mathrm{x}^3}{\mathrm{e^x}-1}\,\mathrm{dx} \quad (7)$$

where θ is the Debye temperature, n = 20 is the number of atoms in the formula unit, R is the gas constant. The volume dependence of the Debye temperature and Grüneisen parameter are described by following equations, where q is the dimensionless power mode parameter:

$$\theta = \theta_0 \exp\left(\frac{\gamma_0 - \gamma}{q}\right) \quad (8)$$

$$\gamma = \gamma_0 \left(\frac{V}{V_0}\right)^q \quad (9)$$

In this approach, six parameters V_0, K_{T0}, K'_{T0}, γ_0, θ_0 and q can be determined by the fitting of the $P-V-T$ data. We recognized that some scattering in the present $P-V-T$ data and limited coverage of low-P high-T region of $P-T$ diagram (Fig.3) related to phase transition from Na-maj to Na-px make it difficult to constrain all six parameters by the simultaneous fitting. Therefore, fitting have been carried out with θ_0 fixed at 890 K. This value was calculated from sound velocities using the following equations based on Debye's lattice vibrational model (Poirier, 2000):

$$\theta = \frac{\hbar}{k_B}\left(\frac{6\pi^2 n Z}{V}\right)^{1/3} \quad (10)$$

where $\hbar$ is the Planck's constant ($\hbar = h/2\pi$), k_B is the Boltzmann's constant, Z = 8 is the number of chemical formula in unit cell, V is the unit cell volume and $\bar{u}$ is the Debye average velocity, reported by Pacalo et al. (1992). Probably for orthosilicates measured calorimetric Debye temperature values are near 950 K and calculated elastic θ_0 would be lower (Kieffer, 1979). For example, the elastic θ_0 for grossular and pyrope are 821 and 794 K, respectively, while calorimetric θ_0 calculated from the heat capacity would be close to 1000 K (Kieffer, 1980). The θ_0 value may affect the fitted other parameters in MGD EoS fittings. To check the possible dependence we decided to show fitted parameters for θ_0 = 1000 K. However, when θ_0 is varied by ± 100 K, the results still agree within the error bars (see below). Parameter q was also fixed at 1, because for a wide range of materials, the volume dependence of Grüneisen parameter is consistent with q equal to 1 (Stixrude and Bukowinski, 1990) and the unit-cell volume and bulk modulus of garnets (i.e. grossular) are almost unaffected when q values vary from 0 to 1.4 (Gréaux et al., 2011).

The results of the MGD EoS fit are summarized in Table 3 and Figure 8. From the simple thermodynamic identity $(\partial K_T/\partial T)_V = (\partial K_T/\partial T)_P + \alpha K_T(\partial K_T/\partial T)_T$ and using the data at ambient conditions (K_T = 184 GPa, $K'_{0,300} = (\partial K_T/\partial T)_T$ = 3.8, $(\partial K_T/\partial T)$ = -0.023 GPa K^{-1} and $\alpha = 3.23 \times 10^{-5}$ K^{-1}) we obtain $(\partial K_T/\partial T)_V$ = 0. As it was shown by Wang et al. (1998) the fact that $(\partial KT/\partial T)_V$ = 0 indicates that thermal pressure is independent on volume and therefore $\Delta P_{th}(V,T) = \Delta P_{th}(V_0,T)$. This is better illustrated in Fig. 8, where thermal pressures remain essentially constant over a wide range of volume and temperature. As it can be seen from the Fig. 8 this fitting leads to almost flat trends so that ΔP_{th} remains independent of cell volume. The solid lines in Fig. 8 represents theoretical thermal pressure obtained by fitting the equation 6 and 7 with experimental data while the points demonstrate

observed values of thermal pressure. The observed values of ΔP_{th} were obtained by subtracting $P(V,300)$ calculated using the fitted BM EoS at 300 K from observed $P(V,T)$ in the experiment. The close agreement between the calculated and the observed values of the thermal pressure indicates that the parameters of the equation of state are accurate.

The V_0 = 1475.9 Å^3, K_T = 184 GPa and K'_T = 3.8 were fixed during the fitting MGD EoS to present data as more accurate parameters obtained in the HTBM EoS. Similarly to the HTBM fitting this approach leads to the minimum RMS misfit of delta pressure ($P_{obs} - P_{cal}$) and corresponds to more accurate calculation. We performed two independent series of calculations. When MGD EoS is fitted to the present $P-V-T$ data at fixed q = 1 and θ_0 = 890 K, we obtained γ_0 = 1.35 (1). Fitting the present data at θ_0 = 1000 K yields γ_0 = 1.37 (1). Thus, the γ_0 is almost unaffected by changes in θ_0 values up to 200 K. The obtained values of γ_0 = 1.35– 1.37 (q = 1) are in good agreement with the value of γ_0 = 1.41 reported by *ab initio* simulation for Mg-majorite (Stixrude and Lithgow-Bertelloni, 2005). They are also similar to γ_0 for other garnet end-members (e.g., pyrope, Zou et al. (2012) and grossular, Gréaux et al. (2011)). The value of the Grüneisen parameter is also typical for mantle phases, γ_0 = 1.0– 1.6 (e.g. Poirier, 2000) so the parameters obtained by fitting of MGD EoS to the present data seem to be reliable.

4. Summary and conclusions

Using synchrotron X-ray diffraction and Kawai-type multi-anvil apparatus, $P-V-T$ measurements on Na-maj have been carried out at pressures between 3 and 21 GPa and temperatures up to 1673 K. Previous data on Na-maj were limited by studies at ambient conditions.

The fit of the present $P-V-T$ data to the HTBM EoS yielded V_0 = 1475.9 Å^3, $K_{0,300}$ = 184 (4) GPa, $K'_{0,300}$ = 3.8 (6), $(\partial K_{0,T}/\partial T)$ = -0.023 (5) GPa K^{-1}, and parameters for thermal expansion coefficient ($\alpha = a + bT$): a = 3.18 (16) × 10^{-5} K^{-1} and b = 0.18 (21) × 10^{-8} K^{-2}. Fitting of the present data to the MGD EoS at θ_0 = 890 K and q = 1 yields γ_0 = 1.35 (1). On the basis of those studies we adopt $K'_{0,300}$ close to 3.8– 4.4 and propose the bulk modulus of $K_{0,300}$ = 180– 184 GPa and Grüneisen parameter of γ_0 = 1.35– 1.37.

Finally, the obtained values of the thermoelastic parameters for Na-maj are higher than for any other garnets, while the cell volume shows the lowest value. Along with previous measurements on the high pressure minerals, obtained thermoelastic parameters of Na-majorite (and further for other garnet end-members, e.g., knorringite) will be used for estimating pressures in natural majoritic garnets.

Acknowledgments

We thank the reviewers for critical comments and suggestions. This work was supported by the Ministry of education and science of Russian Federation, project No 14.B25.31.0032, integration project of Siberian Branch of Russian Academy of Science No 97 for 2012-2014, Russian Foundation for Basic Research (grants Nos 12-05-33008-a and 12-05-31351-mol-a), Ministry of Education and Science of Russian Federation (project No 14.B25.31.0032), grant-in-Aid for Young Scientists No 21684032 and grant-in-Aid for Scientific Research on Innovative Areas No 20103003 from Japan Society for Promotion of Science. The project was conducted as a part of the Global Center-of-Excellence Program 'Global Education and research Center for Earth and Planetary dynamics' at Tohoku University. Experiments were conducted under 'SPring-8' general research proposals Nos 2011B1091, 2012A1416, 2012B1289 and Photon Factory No 2012G031.

References

Akaogi, M., Akimoto, S., 1977. Pyroxene-garnet solid-solution equilibria in the systems $Mg_4Si_4O_{12}$-$Mg_3Al_2Si_3O_{12}$ and $Fe_4Si_4O_{12}$-$Fe_3Al_2Si_3O_{12}$ at high pressures and temperatures. Physics of the Earth and Planetary Interiors, 15, 90-106.

Anderson, D.L., Bass, J.D., 1984. Mineralogy and composition of the upper mantle. Geophysical Research Letters, 11, 637-640.

Bindi, L., Dymshits, A.M., Bobrov, A.V., Litasov, K.D., Shatskiy, A.F., Ohtani, E., Litvin, Y.A., 2011. Crystal chemistry of sodium in the Earth's interior: The structure of $Na_2MgSi_5O_{12}$ synthesized at 17.5 GPa and 1700°C. American Mineralogist, 96, 447-450.

Bobrov, A.V., Kojitani, H., Akaogi, M., Litvin, Y.A., 2008a. Phase relations on the diopside–jadeite–hedenbergite join up to 24 GPa and stability of Na-bearing majoritic garnet. Geochimica et Cosmochimica Acta, 72, 2392-2408.

Bobrov, A.V., Litvin, Y.A., Bindi, L., Dymshits, A.M., 2008b. Phase relations and formation of sodium-rich majoritic garnet in the system $Mg_3Al_2Si_3O_{12}$–$Na_2MgSi_5O_{12}$ at 7.0 and 8.5 GPa. Contributions to Mineralogy and Petrology, 156, 243-257.

Chopelas, A., 2006. Modeling the thermodynamic parameters of six endmember garnets at ambient and high pressures from vibrational data. Physics and Chemistry of Minerals, 33, 363-376.

Collerson, K.D., Williams, Q., Kamber, B.S., Omori, S., Arai, H., Ohtani, E., 2010. Majoritic garnet: A new approach to pressure estimation of shock events in meteorites and the encapsulation of sub-lithospheric inclusions in diamond. Geochimica et Cosmochimica Acta, 74, 5939-5957.

Dorogokupets, P.I., Dewaele, A., 2007. Equations of state of MgO, Au, Pt, NaCl-B1, and NaCl-B2: Internally consistent high-temperature pressure scales. High Pressure Research, 27, 431-446.

Dymshits, A.M., Bobrov, A.V., Bindi, L., Litvin, Y.A., Litasov, K.D., Shatskiy, A.F., Ohtani, E., 2013. Na-bearing majoritic garnet in the $Na_2MgSi_5O_{12}$–$Mg_3Al_2Si_3O_{12}$ join at 11–20 GPa: Phase relations, structural peculiarities and solid solutions. Geochimica et Cosmochimica Acta, 105, 1-13.

Gasparik, T., 1989. Transformation of enstatite− diopside− jadeite pyroxenes to garnet. Contributions to Mineralogy and Petrology, 102, 389-405.

Gréaux, S., Kono, Y., Nishiyama, N., Kunimoto, T., Wada, K., Irifune, T., 2011. P–V–T equation of state of $Ca_3Al_2Si_3O_{12}$ grossular garnet. Physics and Chemistry of Minerals, 38, 85-94.

Gwanmesia, G.D., Liu, J., Chen, G., Kesson, S., Rigden, S.M., Liebermann, R.C., 2000. Elasticity of the pyrope ($Mg_3Al_2Si_3O_{12}$)-majorite ($MgSiO_3$) garnets solid solution. Physics and Chemistry of Minerals, 27, 445-452.

Hamilton, D.L., Henderson, C.M.B., 1968. The preparation of silicate compositions by a gelling method. Mineralogical Magazine, 36, 832-838.
Harte, B., 2010. Diamond formation in the deep mantle: the record of mineral inclusions and their distribution in relation to mantle dehydration zones. Mineralogical Magazine, 74, 189-215.
Hazen, R.M., Downs, R.T., Conrad, P.G., Finger, L.W., Gasparik, T., 1994. Comparative compressibilities of majorite-type garnets. Physics and Chemistry of Minerals, 21, 344-349.
Holland, T.J.B., Redfern, S.A.T., 1997. Unit cell refinement from powder diffraction data: The use of regression diagnostics. Mineralogical Magazine, 61, 65-77.
Hunt, S.A., Dobson, D.P., Li, L., Weidner, D.J., Brodholt, J.P., 2010. Relative strength of the pyrope–majorite solid solution and the flow-law of majorite containing garnets. Physics of the Earth and Planetary Interiors, 179, 87-95.
Irifune, T., Ringwood, A.E., 1987. Phase transformations in a harzburgite composition to 26 GPa: implications for dynamical behaviour of the subducting slab. Earth and Planetary Science Letters, 86, 365-376.
Ita, J., Stixrude, L., 1992. Petrology, elasticity, and composition of the mantle transition zone. Journal of Geophysical Research: Solid Earth, 97, 6849-6866.
Jackson, I., Rigden, S.M., 1996. Analysis of P-V-T data: constraints on the thermoelastic properties of high-pressure minerals. Physics of the Earth and Planetary Interiors, 96, 85-112.
Katsura, T., Funakoshi, K.-i., Kubo, A., Nishiyama, N., Tange, Y., Sueda, Y.-i., Kubo, T., Utsumi, W., 2004. A large-volume high-pressure and high-temperature apparatus for in situ X-ray observation,'SPEED-Mk. II'. Physics of the Earth and Planetary Interiors, 143, 497-506.
Kieffer, S.W., 1979. Thermodynamics and lattice vibrations of minerals: 1. Mineral heat capacities and their relationships to simple lattice vibrational models. Reviews of Geophysics, 17, 1-19.
Kieffer, S.W., 1980. Thermodynamics and lattice vibrations of minerals: 4. Application to chain and sheet silicates and orthosilicates. Reviews of Geophysics, 18, 862-886.
Kiseeva, E.S., Yaxley, G.M., Stepanov, A.S., Tkalčić, H., Litasov, K.D., Kamenetsky, V.S., 2013. Metapyroxenite in the mantle transition zone revealed from majorite inclusions in diamonds. Geology, 41, 883-886.
Litasov, K.D., Dorogokupets, P.I., Ohtani, E., Fei, Y., Shatskiy, A., Sharygin, I.S., Gavryushkin, P.N., Rashchenko, S.V., Seryotkin, Y.V., Higo, Y., 2013. Thermal equation of state and thermodynamic properties of molybdenum at high pressures. Journal of Applied Physics, 113, 093507.
Litasov, K.D., Ohtani, E., 2009. Phase relations in the peridotite–carbonate–chloride system at 7.0–16.5 GPa and the role of chlorides in the origin of kimberlite and diamond. Chemical Geology, 262, 29-41.
Milman, V., Akhmatskaya, E., Nobes, R., Winkler, B., Pickard, C., White, J., 2001. Systematic ab initio study of the compressibility of silicate garnets. Acta Crystallographica Section B: Structural Science, 57, 163-177.
Pacalo, R.E.G., Weidner, D.J., Gasparik, T., 1992. Elastic properties of sodium-rich majorite garnet. Geophysical Research Letters, 19, 1895-1898.
Poirier, J.P. (Ed.), 2000. Introduction to the Physics of the Earth's Interior. Cambridge Univ. Press, Cambridge, UK, 312 pp.
Simakov, S.K., Bobrov, A.V., 2008. Garnet-pyroxene barometry for the assemblages with Na-bearing majoritic garnet. Doklady Earth Sciences, 420, 667-669.
Sinogeikin, S.V., Bass, J.D., 2002. Elasticity of Majorite and a Majorite-Pyrope solid solution to high pressure: Implications for the Transition Zone. Geophysical Research Letters, 29, 41-44.
Sobolev, N.V., Lavrent'ev, J.G., 1971. Isomorphic sodium admixture in garnets formed at high pressures. Contributions to Mineralogy and Petrology, 31, 1-12.
Sokolova, T.S., Dorogokupets, P.I., Litasov, K.D., 2013. Self-consistent pressure scales based on the equations of state for ruby, diamond, MgO, B2-NaCl, as well as Au, Pt and other metals to 4 Mbars and 3000 K. Russian Geology and Geophysics, 54, 181–199.

Stachel, T., 2001. Diamonds from the asthenosphere and the transition zone. European Journal of Mineralogy, 13, 883-892.

Stixrude, L., Bukowinski, M., 1990. Fundamental thermodynamic relations ans silicate melting with implications for the constitution of D'. Geophysical Research Letters, 95, 19311-19325.

Stixrude, L., Lithgow‐Bertelloni, C., 2005. Mineralogy and elasticity of the oceanic upper mantle: Origin of the low‐velocity zone. Journal of Geophysical Research: Solid Earth (1978–2012), 110, doi: 10.1029/2004JB002965.

Suzuki, A., Ohtani, E., Terasaki, H., Nishida, K., Hayashi, H., Sakamaki, T., Shibazaki, Y., Kikegawa, T., 2011. Pressure and temperature dependence of the viscosity of a $NaAlSi_2O_6$ melt. Physics and Chemistry of Minerals, 38, 59-64.

Utsumi, U., Funakoshi, K., Urakawa, S., Yamakata, M., Tsuji, K., Konishi, H., 1998. SPring-8 beamlines for high pressure science with multi-anvil apparatus. Review of High Pressure Science and Technology, 7, 1484–1486.

Vinograd, V.L., Dymshits, A.M., Winkler, B., Bobrov, A.V., 2011. Computer simulation of Na-bearing majoritic garnet. Doklady Earth Sciences, 441, 1508-1511.

Wang, Y., Weidner, D.J., Zhang, J., Gwanrnesia, G.D., Liebermann, R.C., 1998. Thermal equation of state of garnets along the pyrope-majorite join. Physics of the Earth and Planetary Interiors, 105, 59-71.

Yang, H., Konzett, J., Frost, D.J., Downs, R.T., 2009. X-ray diffraction and Raman spectroscopic study of clinopyroxenes with six-coordinated Si in the $Na(Mg_{0.5}Si_{0.5})Si_2O_6$-$NaAlSi_2O_6$ system. American Mineralogist, 94, 942-949.

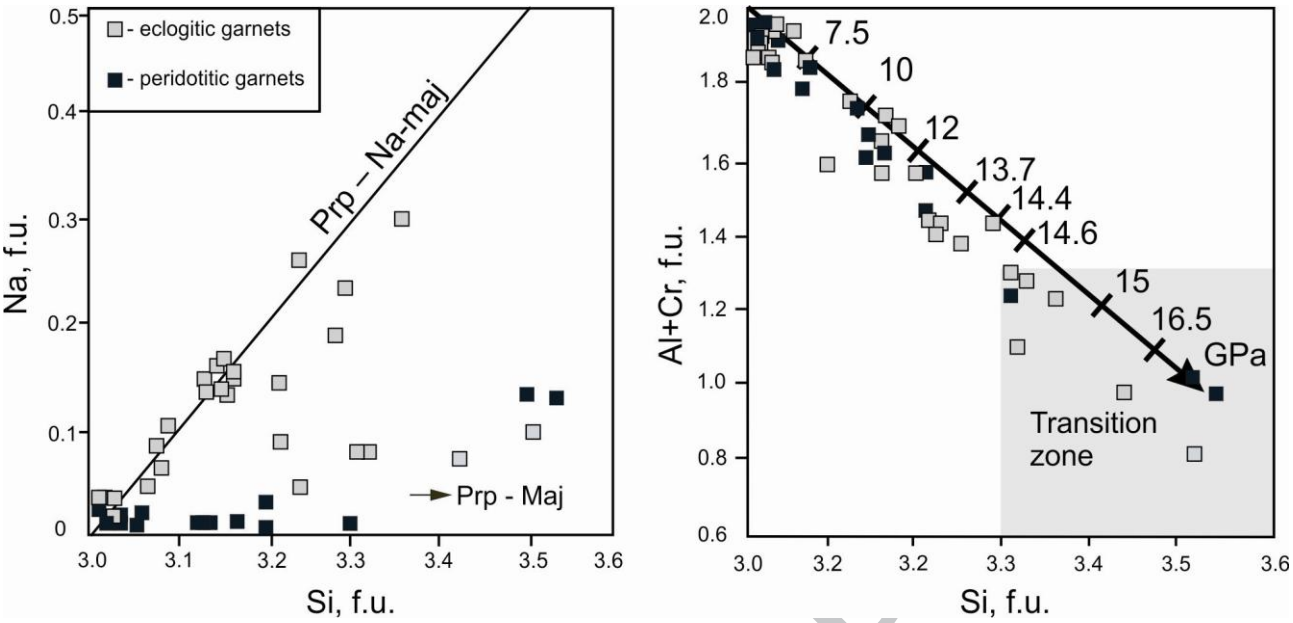

Fig. 1. Na-bearing majoritic garnets compositions from inclusions in diamonds (Moore and Gurney, 1985; Davies et al., 1999a; Davies et al., 1999b; Stachel, 2001; Pokhilenko et al., 2004; Harte and Cayzer, 2007; Shatskii et al., 2010). Pressure scale based on experimental data interpreted by Stachel (2001).

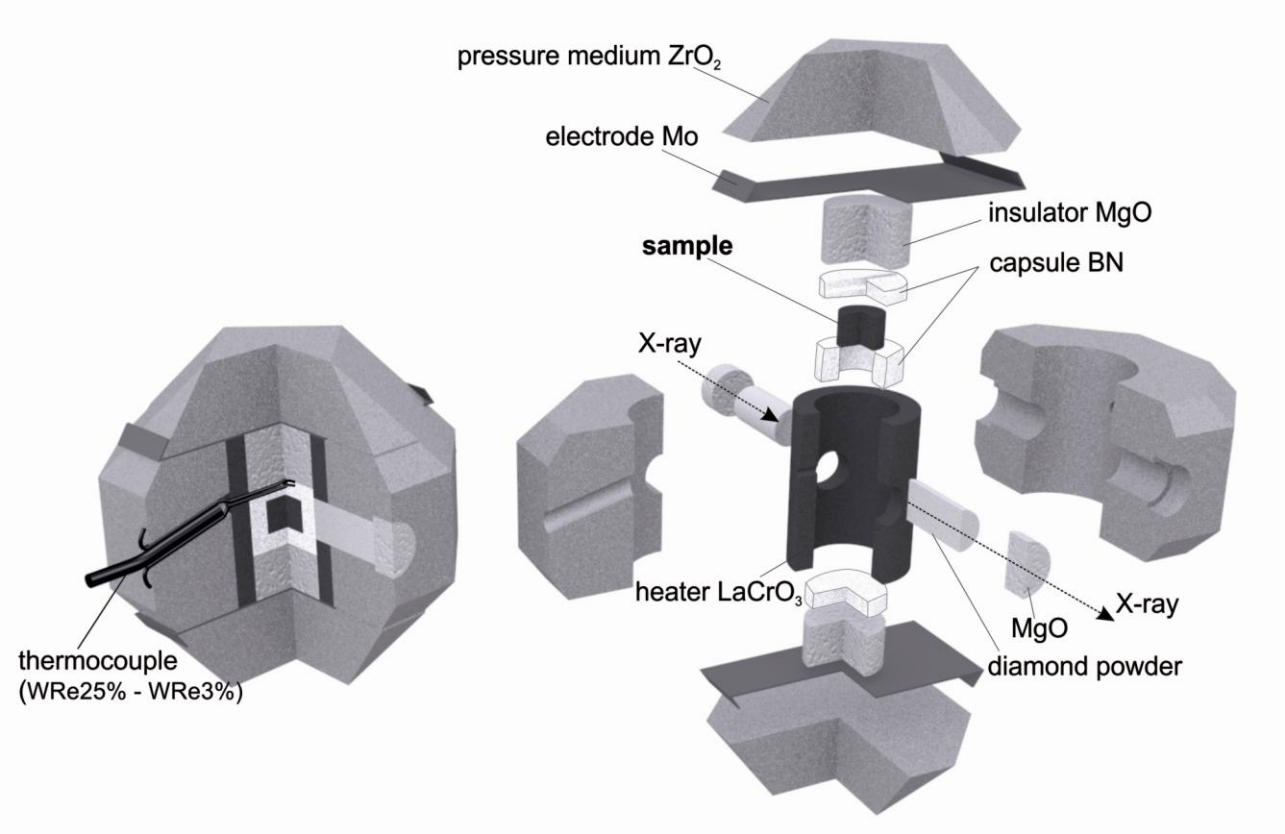

Fig. 2. Schematic illustration of the 3.5 TEL high-pressure cell used for experiments.

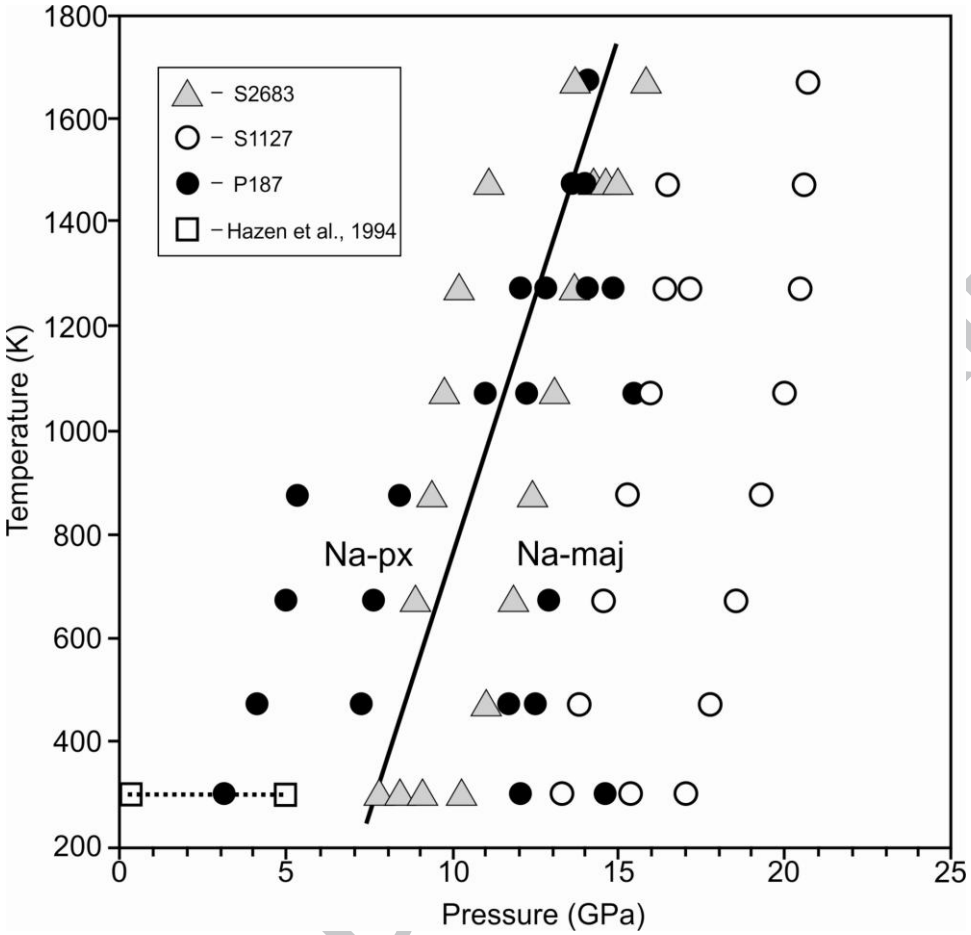

Fig. 3. Pressure–temperature conditions of *in situ* X-ray diffraction experiments. The pressures were calculated using Au EoS (by Dorogokupets and Dewaele (2007); Sokolova et al. (2013)). Dotted line covers the conditions studied by Hazen et al. (1994). Solid line illustrates Na-px - Na-maj transition (Dymshits et al., 2010).

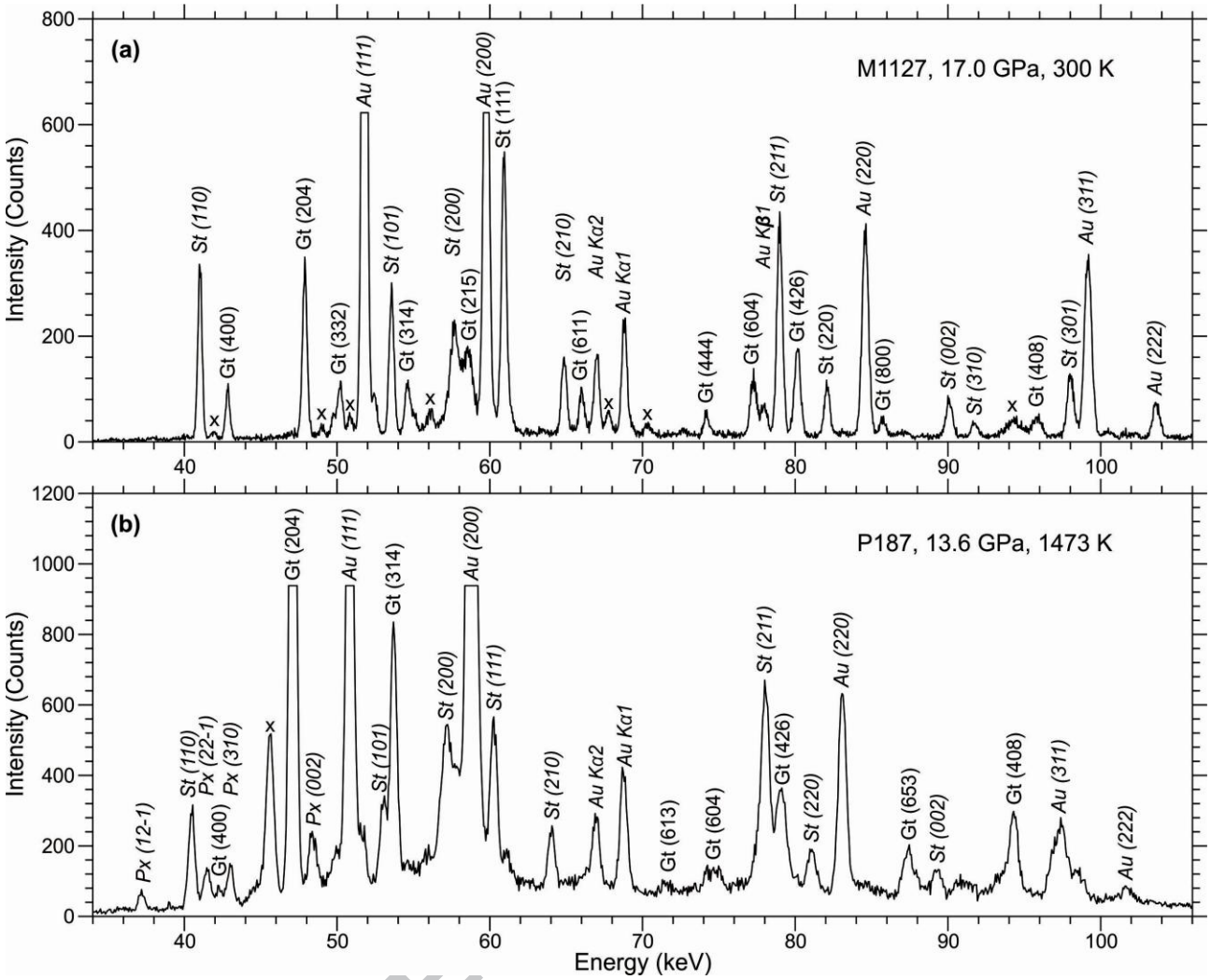

Fig. 4. Examples of X-ray diffraction pattern collected for Na-majorite (Na-maj) in Na-maj stability field (a) and Na-px stability field (b). Px – Na-px; Gt – Na-maj; St – stishovite; Au – gold; X – unidentified picks.

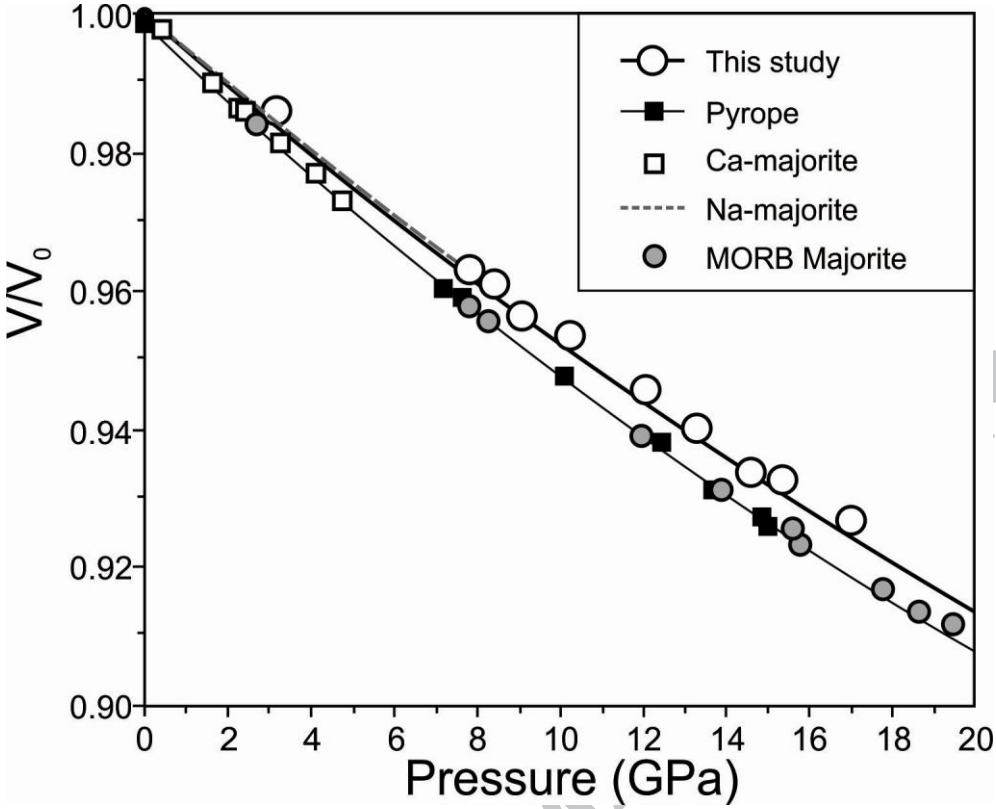

Fig. 5. Comparison of room temperature compression (V/V_0) data and compressibility curve for Na-majorite (this study) and other garnets: pyrope (Zou et al., 2012), calcium-bearing majorite $(Ca_{0.49}Mg_{2.51})(MgSi)Si_3O_{12}$ and sodium majorite $(Na_{1.88}Mg_{1.12}(Mg_{0.06}Si_{1.94})Si_3O_{12}$ (Hazen et al., 1994), synthetic MORB majorite (Nishihara et al., 2005).

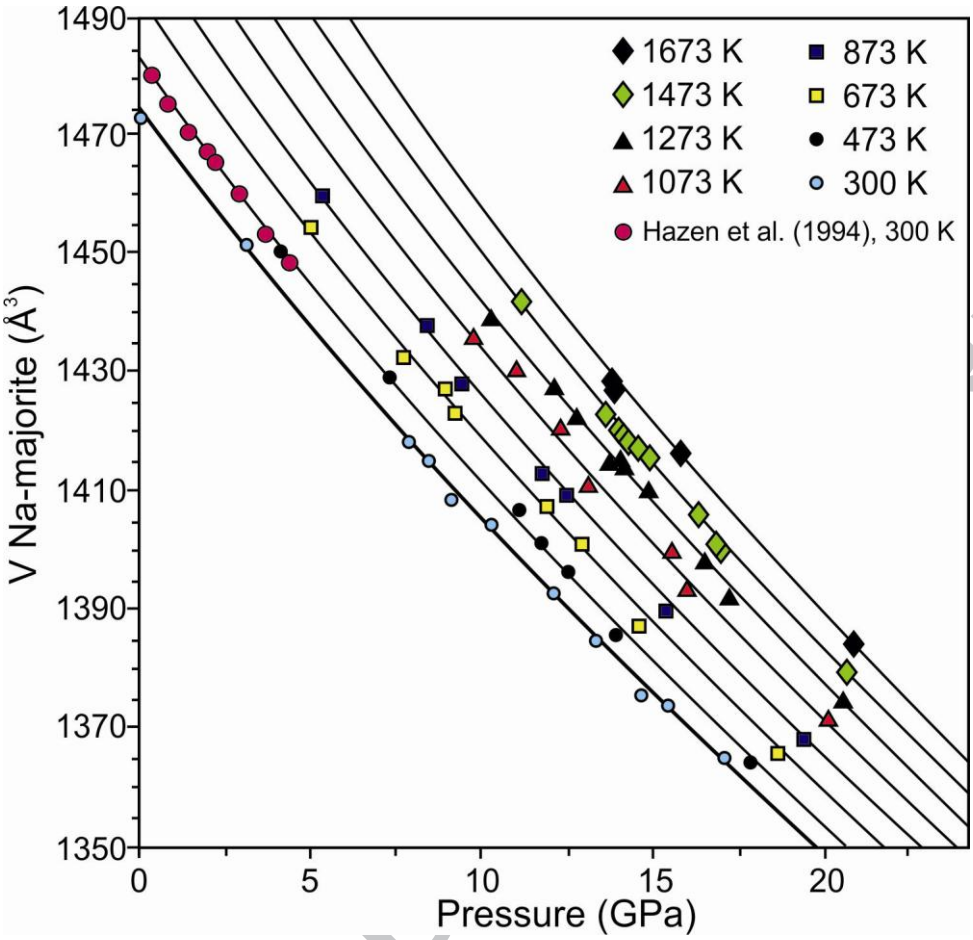

Fig. 6. $P-V-T$ relations of Na-majorite obtained from the present study V_0 = 1475.9 Å^3; $K_{0,300}$ = 184 (3) GPa, $K'_{0,300}$ = 3.8 (6), $(\partial K_{0,T}/\partial T)$ = -0.023 (5) GPa K^{-1}, a = 3.18 (16) × 10^{-5} K^{-1}, and b = 0.18 (21) × 10^{-8} K^{-2}, where $\alpha = a + bT$ is the volumetric thermal expansion coefficient The solid lines represent isothermal compression curves at various temperatures calculated by using the yielded thermoelastic parameters of the present study. For comparison, open circles are plotted after Hazen et al. (1994) at 300 K.

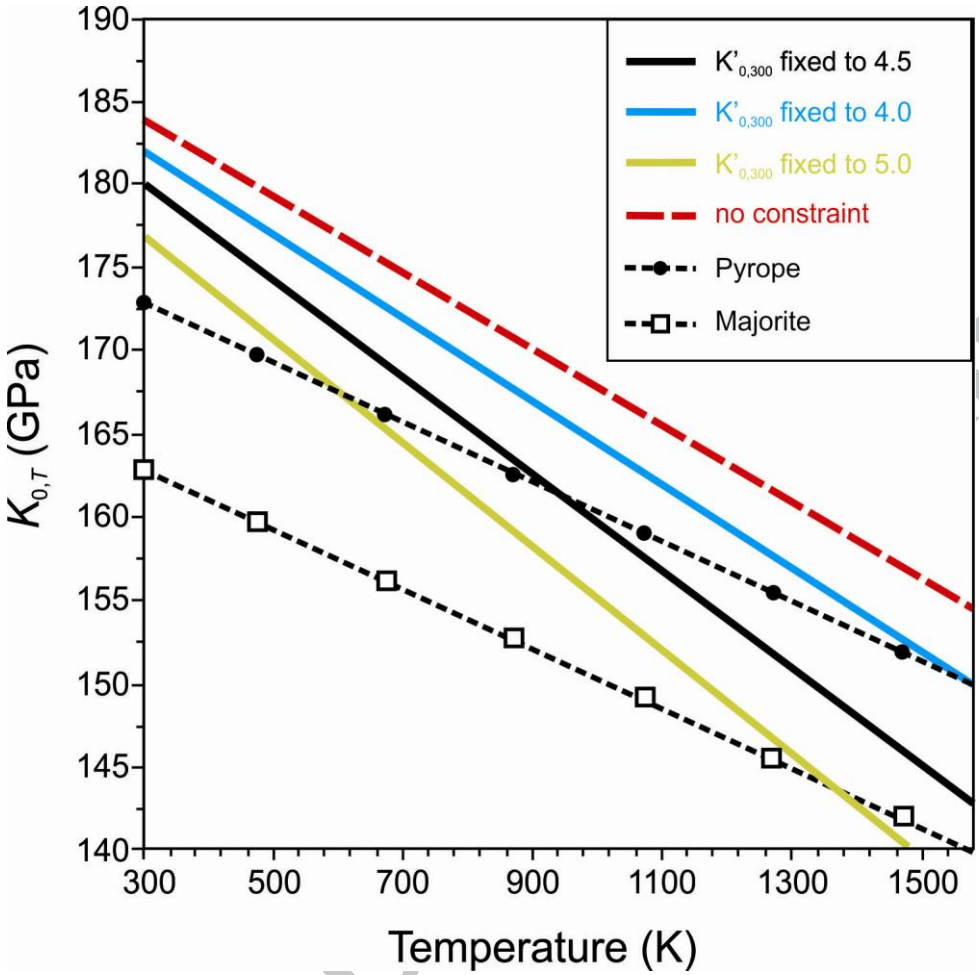

Fig. 7. Isothermal bulk modulus $K_{0,T}$ against temperature. Solid lines represent our data for different fixed values of $K'_{0,300}$ (4.0, 4.5 and 5.0) as well as red dashed line for no constraint on the elastic parameters ($K_{0,T}$ = 184 GPa and $K_{0,300}$ = 3.8). Circles and squares symbolize the previous studies by (Hunt et al., 2010).

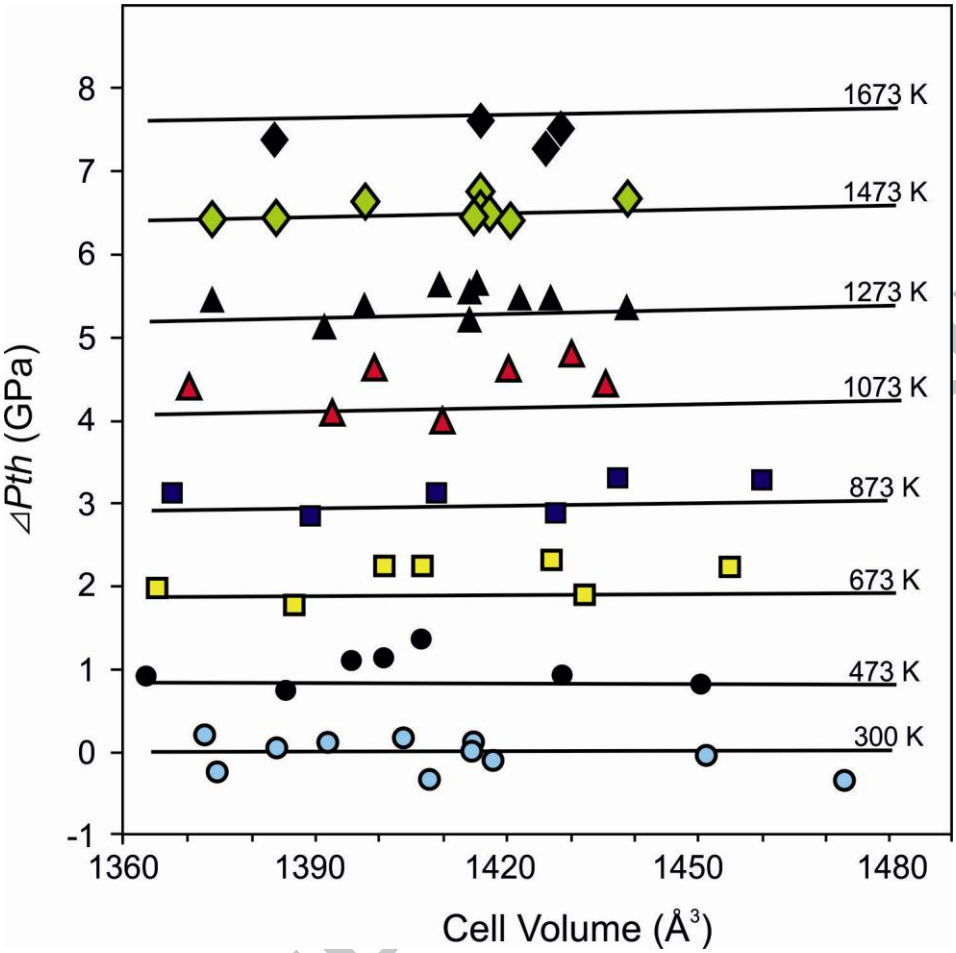

Fig. 8. Thermal pressure (*ΔPth*) vs. cell volume for Na-majorite. Solid lines are thermal pressures calculated using MGD EoS fit to the present data. Symbols are same as in Figure 6.

Table 1

Unit cell parameters of Na-majorite at various $P-T$ conditions

V_{Au} (Å^3)	P (GPa)	T (K)	$a_{Na\text{-}maj}$ (Å)	$V_{Na\text{-}maj}$ (Å^3)	V_{Au} (Å^3)	P (GPa)	T (K)	$a_{Na\text{-}maj}$ (Å)	$V_{Na\text{-}maj}$ (Å^3)
				Run P187	62.96 (2)	19.3 (1)	873	11.1011 (3)	1367.88 (12)
65.66 (3)	14.0 (1)	1473	11.2416 (3)	1420.65 (13)	62.82 (2)	18.6 (1)	673	11.0940 (3)	1365.52 (12)
65.68 (4)	14.0 (1)	1473	11.2414 (4)	1420.59 (12)	62.69 (3)	17.8 (1)	473	11.0900 (3)	1363.94 (12)
65.80 (3)	13.6 (2)	1473	11.2481 (3)	1423.11 (13)	62.60 (3)	17.0 (1)	300	11.0920 (3)	1364.70 (11)
65.20 (1)	14.1 (1)	1273	11.2271 (3)	1415.14 (12)	63.01 (3)	15.4 (1)	300	11.1165 (3)	1373.48 (12)
63.87 (4)	12.1 (1)	300	11.1670 (3)	1392.47 (12)	64.26 (3)	17.2 (2)	1273	11.1640 (4)	1391.68 (13)
65.35 (2)	12.2 (1)	1073	11.2460 (3)	1420.67 (12)	64.87 (2)	16.5 (1)	1473	11.2000 (4)	1405.91 (15)
65.62 (1)	12.8 (1)	1273	11.2460 (3)	1422.31 (12)	64.48 (4)	16.4 (1)	1273	11.1820 (4)	1398.06 (14)
64.29 (4)	11.7 (2)	473	11.1900 (4)	1401.17 (13)	64.23 (5)	15.9 (2)	1073	11.1681 (4)	1393.05 (13)
65.77 (4)	11.0 (1)	1073	11.2680 (3)	1430.50 (12)	64.03 (4)	15.3 (1)	873	11.1580 (4)	1389.64 (13)
65.87 (4)	12.0 (1)	1273	11.2589 (3)	1427.23 (12)	63.86 (4)	14.6 (1)	673	11.1520 (4)	1387.16 (13)
63.20 (2)	14.6 (1)	300	11.1210 (3)	1375.27 (12)	63.70 (5)	13.8 (1)	473	11.1486 (4)	1385.63 (13)
64.36 (4)	15.5 (2)	1073	11.1860 (4)	1399.62 (15)	63.54 (2)	13.3 (1)	300	11.1458 (4)	1384.62 (13)
64.96 (4)	14.8 (1)	1273	11.2131 (3)	1409.89 (12)					*Run S2683*
65.55 (5)	14.4 (2)	1473	11.2351 (3)	1418.19 (12)	66.71 (3)	11.1 (1)	1473	11.2992 (3)	1442.70 (13)
66.18 (2)	13.9 (3)	1673	11.2559 (3)	1426.43 (13)	66.53 (2)	10.2 (1)	1273	11.2900 (4)	1439.25 (15)
65.64 (2)	14.1 (2)	1473	11.2396 (3)	1419.88 (12)	66.19 (3)	9.8 (1)	1073	11.2820 (4)	1436.07 (16)
65.19 (2)	14.1 (1)	1273	11.2252 (3)	1414.44 (12)	65.85 (3)	9.4 (1)	873	11.2617 (3)	1427.98 (12)
64.34 (3)	12.9 (1)	673	11.1900 (3)	1400.98 (12)	65.56 (3)	8.9 (1)	673	11.2611 (3)	1427.48 (13)
64.07 (3)	12.5 (1)	473	11.1760 (3)	1396.09 (12)	65.10 (2)	7.8 (1)	300	11.2350 (3)	1418.19 (12)
66.18 (2)	8.4 (2)	873	11.2860 (4)	1437.65 (13)	64.92 (2)	8.4 (1)	300	11.2270 (3)	1414.95 (12)
65.97 (4)	7.6 (1)	673	11.2730 (3)	1432.58 (12)	64.72 (2)	9.1 (1)	300	11.2092 (3)	1408.36 (12)
65.65 (2)	7.2 (1)	473	11.2640 (3)	1429.10 (12)	64.38 (1)	10.2 (1)	300	11.1988 (3)	1404.22 (12)
67.33 (3)	5.3 (3)	873	11.3440 (3)	1460.08 (13)	64.48 (2)	11.0 (1)	473	11.2059 (4)	1406.84 (14)
66.93 (3)	5.0 (2)	673	11.3310 (3)	1454.93 (13)	64.64 (2)	11.8 (1)	673	11.2063 (40	1407.31 (12)
66.74 (4)	4.1 (2)	473	11.3200 (4)	1450.62 (14)	64.87 (3)	12.4 (1)	873	11.2120 (3)	1409.33 (12)
66.67 (2)	3.1 (1)	300	11.3230 (4)	1451.65 (14)	65.09 (4)	13.1 (1)	1073	11.2154 (3)	1410.61 (13)
67.93 (1)	0	300	11.3855 (4)	1475.88 (16)	65.31 (3)	13.7 (1)	1273	11.2250 (3)	1414.36 (12)
				Run M1127	65.58 (4)	14.3 (1)	1473	11.2390 (3)	1419.42 (12)
64.00 (3)	20.7 (1)	1673	11.1442 (3)	1384.00 (12)	65.46 (3)	14.6 (1)	1473	11.2326 (3)	1417.23 (12)
63.67 (2)	20.6 (1)	1473	11.1230 (3)	1379.66 (12)	65.35 (4)	15.0 (1)	1473	11.2295 (3)	1416.02 (12)
63.34 (2)	20.5 (1)	1273	11.1180 (3)	1374.24 (12)	65.51 (3)	15.8 (1)	1673	11.2298 (3)	1416.17 (12)
63.12 (2)	20.0 (1)	1073	11.1090 (3)	1371.01 (12)	65.24 (4)	13.7 (1)	1673	11.2622 (3)	1428.47 (12)

Numbers in parenthesis represent the relative error calculated for *a, V* and *P*. Pressure was calculated from the Eos of Au (Dorogokupets and Dewaele, 2007; Sokolova et al., 2013).

Table 2. The results of the fitting by the HTBM EoS of Na-majorite, compared to previous works on other majorite-type and some other garnets

	V_0 (Å^3)	$K_{0,300}$ (GPa)	$K'_{0,300}$	$(\partial K_{0,T}/\partial T)$ (GPa K^{-1})	$\alpha_{0,300}$ (10^{-5} K^{-1})	a (10^{-5} K^{-1})	b (10^{-8} K^{-2})
1) Na-maj	1475.9*	182 (1)	4*	-0.025 (4)	3.27 (17)	3.20 (14)	0.24 (20)
	1475.9*	177 (1)	5*	-0.031 (3)	3.48 (21)	3.31 (14)	0.58 (24)
	1475.9*	**184 (4)**	**3.8 (6)**	**-0.023 (5)**	**3.23 (15)**	**3.18 (16)**	**0.18 (21)**
	1475.9*	180*	4.3 (1)	-0.026 (3)	3.37 (15)	3.27 (13)	0.32 (24)
	1476 (1)	186 (6)	3.6 (7)	-0.023 (5)	3.22 (18)	3.17 (16)	0.16 (26)
300K BM EoS							
	1476 (1)	184 (3)	4*				
	1475.9*	180 (5)	4.5 (9)				
	1476 (1)	181 (9)	4 (1)				
2) $NaMaj_{95}Maj_5$		173.5					
3) $NaMaj_{94}Maj_6$	1485.5 (3)	192	4	–		–	–
4) Ca-maj	1547.0 (3)	165					
5) Maj	1520.0	165 (3)	4.2 (3)				
6) Maj garnet	1574.1	173 (1)	4*	-0.022 (5)		2.0 (3)	1.0 (5)
7) $Prp_{50}Maj_{50}$		166 (3)	4.2 (3)	-0.022 (2)			
8) Prp_{100}	1500.4 (2)	167	4.6	-0.021 (9)		2.58 (20)	1.02 (46)
9) $Alm_{86}Prp_7Spe_7$	1539.8	177	4*	-0.032	3.1 (7)		
10) And	1754.1	158 (2)	4		3.16 (25)		

1) Na-maj – $Na_2MgSi_5O_{12}$; 2) Na-maj – Pacalo et al. (1992); 3) Na-maj and 4) Ca-maj – $Ca_{0.49}Mg_{3.51}Si_4O_{12}$, Hazen et al. (1994); 5) Maj – $Mg_4Si_4O_{12}$, Stixrude and Lithgow-Bertelloni (2005); 6) majorite synthesized from natural MORB, Nishihara et al. (2005); 7) Sinogeikin and Bass (2002); 8) Prp – $Mg_3Al_2Si_3O_{12}$, Zou et al. (2012); 9) $Alm_{86}Prp_7Spe_7$ – almandine-spessartine solid solution, Fan et al. (2009); 10) And – $Ca_3Al_{0.03}Fe_{1.97}$ Si_3O_{12}, Pavese et al. (2001). The bold line represents the calculation with the more accurate parameters.

* Fixed values during data fitting.

Table 3. Thermoelastic parameters of Na-majorite using Mie– Grüneisen– Debye equation of state

V_0 (Å^3)	1475.9[b]	1475.9[b]
$K_{0,300}$ (GPa)	184[b];	184[b]
$K'_{0,300}$	3.8[b];	3.8[b]
γ_0	1.35 (1);	1.37 (1)
q	1[b];	1[b]
θ (K)	890[a]	1000[b]

[a] Calculated from elastic model (Pacalo et al., 1992); [b] - fixed

Graphical abstract

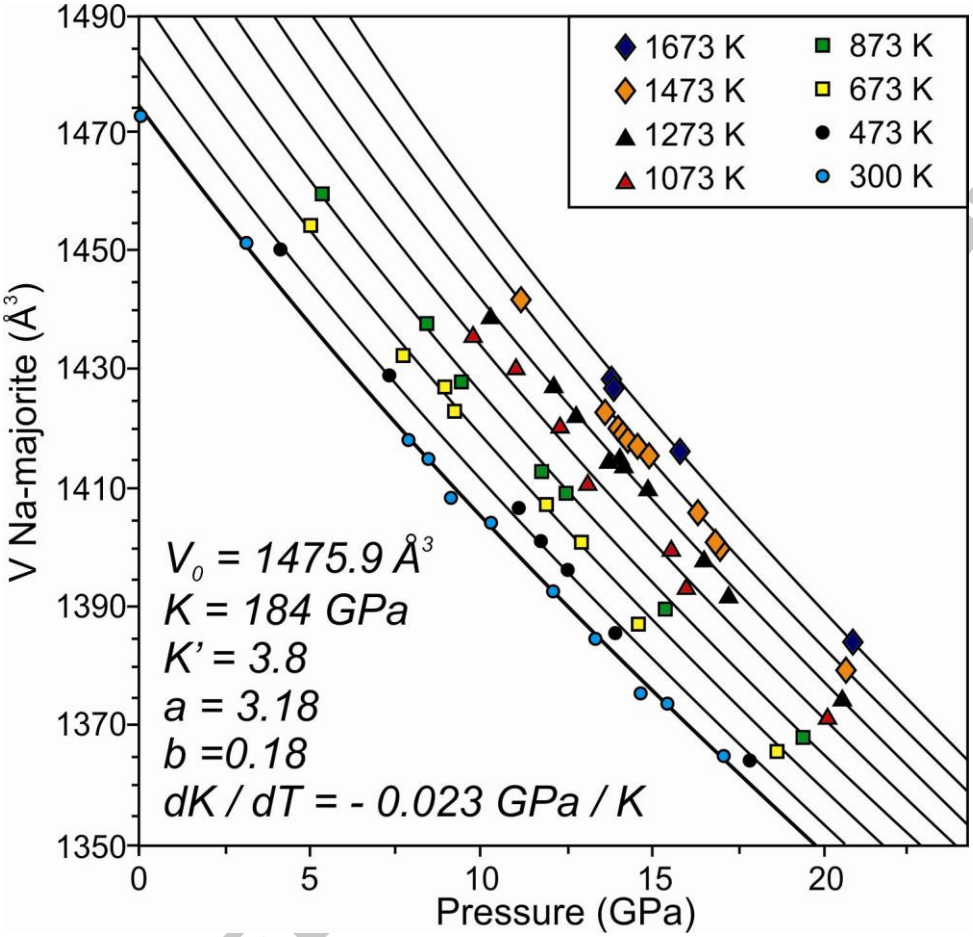

Highlights

- We have conducted *in situ* X-ray diffraction experiments on Na-majorite
- The *P*-*V*-*T* equation of state for Na-majorite to 21 GPa and 1673 K was developed
- Data were fitted using high-temperature Birch–Murnaghan equation of state
- Grüneisen parameter was yielded from the Mie-Grüneisen-Debye equation of state